Published in final edited form as:

Nat Neurosci. 2010 January ; 13(1): 69–75. doi:10.1038/nn.2454.

SLEEPLESS, a Ly–6/Neurotoxin Family Member, Regulates Levels, Localization, and Activity of Shaker

Mark N. Wu[1,5,*], **William J. Joiner**[2,3,*], **Terry Dean**[3,*], **Zhifeng Yue**[2], **Corinne J. Smith**[2], **Dechun Chen**[3], **Toshinori Hoshi**[4], **Amita Sehgal**[2,3], and **Kyunghee Koh**[3,+]

[1]Division of Sleep Medicine, Department of Neurology, University of Pennsylvania, Philadelphia, PA 19104.

[2]Howard Hughes Medical Institute, University of Pennsylvania, Philadelphia, PA 19104.

[3]Department of Neuroscience, University of Pennsylvania, Philadelphia, PA 19104.

[4]Department of Physiology, University of Pennsylvania, Philadelphia, PA 19104.

Abstract

Sleep is a whole–organism phenomenon accompanied by global changes in neural activity. We previously identified SLEEPLESS (SSS) as a novel glycosylphosphatidyl–inositol–anchored protein required for sleep in *Drosophila*. Here, we demonstrate a critical role for SSS in regulating the sleep–modulating potassium channel, Shaker. SSS and Shaker exhibit similar expression patterns in the brain and specifically affect each other's expression levels. *sss* mutants exhibit altered Shaker localization, reduced Shaker current density, and slower Shaker current kinetics. Transgenic expression of *sss* in *sss* mutants rescues defects in Shaker expression and activity cell–autonomously and also suggests that SSS functions in wake–promoting, cholinergic neurons. Importantly, in heterologous cells, SSS accelerates kinetics of Shaker currents and can be co–immunoprecipitated with Shaker, suggesting that SSS interacts with Shaker and modulates its activity. SSS is predicted to belong to the Ly–6/neurotoxin superfamily, suggesting a novel mechanism for regulation of neuronal excitability by endogenous toxin–like molecules.

In mammals, sleep is associated with broad changes in patterns of neuronal activity in the brain. Sleep in fruit flies shares several features of mammalian sleep, such as circadian and homeostatic regulation and increased arousal threshold[1],[2], and is similarly accompanied by broad changes in brain activity[3]. Modulation of neuronal excitability may be an essential component of sleep regulation. This view is supported by several studies demonstrating that mice and flies bearing mutations in genes encoding ion channels and their associated proteins exhibit altered sleep[4]–[8]. For instance, a forward genetic screen led to the

[+]Correspondence should be addressed to (kkoh@mail.med.upenn.edu). .

[5]Present address: Department of Neurology, Johns Hopkins University, Baltimore, MD 21287

[*]These authors contributed equally to this work.

AUTHOR CONTRIBUTIONS M.N.W., W.J.J., and K.K. conceived the study, in close consultation with A.S. M.N.W., W.J.J., T.D., and K.K. planned and performed the experiments, and analyzed the data, with assistance from Z.Y., C.J.S., and D.C. T.H. provided supervision and advice for electrophysiological experiments. The manuscript was written principally by M.N.W. and K.K. with specific sections written by W.J.J. and T.D., and editorial changes made by A.S. and T.H.

identification of a mutation in the gene encoding the canonical voltage–gated potassium channel *Shaker* as the defect underlying a short–sleeping phenotype in *Drosophila*, and targeted disruption of the mammalian *Shaker* ortholog, Kv1.2, also leads to reduced sleep in mice[9,10].

We recently identified a novel gene required for sleep in *Drosophila*, which we named *sleepless (sss)*. *sss* mutants exhibit a severe reduction in sleep and a decreased level of Shaker expression, providing an additional link between sleep and neuronal excitability[11]. However, the mechanism by which SSS regulates Shaker, and thereby neuronal excitability, is not known. The mature SSS protein, ~15 kD in size, is cysteine–rich and covalently linked to the plasma membrane by a glycosylphosphatidyl–inositol (GPI) anchor[11]. We now show that SSS belongs to the Ly–6/neurotoxin superfamily of proteins[12]. This superfamily includes diverse proteins such as secreted signaling molecules and receptors[13–15], as well as snake neurotoxins, which bind to and modulate the activity of various ion channels[12,16].

The predicted Ly–6/neurotoxin domain in SSS suggests at least two distinct potential molecular mechanisms of action. One possibility is that SSS acts as a "proto–toxin," forming a complex with Shaker to control its expression and activity within the same cell. An endogenous toxin–like molecule that regulates Shaker–type channels has been postulated, based on the finding that expression of a Shaker–specific neurotoxin in the endoplasmic reticulum (ER) of mammalian cells increases the surface localization of these channels[17]. Alternatively, since SSS is tethered to the cell surface by a GPI anchor and cleavage of the anchor by phospholipase C results in release of SSS into the media in cultured cells[11], SSS may be a secreted molecule that acts on Shaker indirectly through a receptor–mediated signaling pathway.

Here we present evidence demonstrating a role for SSS as an endogenous toxin–like regulator of Shaker expression, localization, and activity. SSS and Shaker share a similar expression pattern in the *Drosophila* brain, and loss of either SSS or Shaker results in a reduction of the other protein, suggesting that these proteins are required for each other's stability. We show that the ability of SSS to promote sleep localizes to wake–promoting, cholinergic neurons that are distinct from circuitry involved in *sss*–dependent, ether–induced leg–shaking. In *sss* mutants, Shaker appears to be mislocalized, and Shaker currents are smaller and slower. Shaker protein levels as well as current amplitude and kinetics are all rescued in *sss* mutants in a cell–autonomous manner by targeted expression of a *sss* transgene. Finally, in heterologous systems, SSS accelerates kinetics of Shaker currents and can be co–immunoprecipitated with Shaker, suggesting that SSS forms a complex with Shaker and regulates its activity. Together, these results establish SSS as a critical regulator of Shaker channels, defining a novel molecular mechanism for the modulation of neuronal excitability.

RESULTS

Differential rescue of *sss* mutant phenotypes

We previously demonstrated that SSS is markedly enriched in adult brains and that the *sss* mutant sleep phenotype can be rescued using a transgene containing the *sss* genomic

region[11]. To examine the neuronal circuitry required for the sleep phenotype observed in *sss* mutants, we used the Gal4–UAS system to perform targeted rescue of the sss^{P1} mutation[18]. We generated transgenic flies bearing Gal4 under control of the *sss* promoter (*sss*–Gal4, see **Methods**) and found that daily sleep amount is restored to wild–type levels in sss^{P1} mutant flies carrying both the *sss*–Gal4 driver and the UAS–*sss* transgene (Fig. 1a). By crossing flies bearing the *sss*–Gal4 driver to those carrying a UAS–GFP transgene, we found that the *sss*–Gal4 driver expresses broadly, with prominent enrichment in areas such as the mushroom bodies, a region previously shown to be important for sleep regulation,[19],[20] and antennal nerves, in a pattern that overlaps substantially with the SSS immunostaining pattern (compare Supplementary Fig. 1 and Fig. 2, below). Pan–neuronal expression of UAS–*sss* under the control of the *elav*–Gal4 driver also fully rescued the sss^{P1} mutant sleep phenotype (Fig. 1a).

Because both *sss*–Gal4 and *elav*–Gal4 drivers exhibited broad expression patterns, we also examined whether more restricted *sss* expression could rescue the mutant sleep phenotype. We screened a number of Gal4 driver lines with varying expression patterns for their ability to rescue reduced sleep in *sss* mutants. While several drivers promoted strong rescue, they all have broad expression patterns (Supplementary Figs. 2 and 3), making it difficult to pinpoint a specific region required for SSS function. Drivers that promoted more restricted expression patterns were associated with little or no rescue; these included drivers that direct expression in the mushroom bodies, clock cells, and the pars intercerebralis neurons, areas that have been implicated in sleep regulation[19]–[25]. We also examined the effects of overexpressing SSS on sleep amount in wild–type animals. As shown in Supplementary Fig. 4, SSS overexpression using a variety of Gal4 drivers had no significant effect on daily sleep amount.

To examine whether a specific neurotransmitter system underlies the short–sleeping phenotype of *sss* mutants, we employed Gal4 drivers that express in different neurotransmitter systems (Fig. 1b). Expression of *sss* preferentially in cholinergic neurons using *Cha*–Gal4 resulted in strong rescue of the short–sleeping phenotype of sss^{P1} mutants. In contrast, preferential expression of *sss* in glutamatergic or dopaminergic neurons driven by *vGlut*– or *TH*–Gal4 respectively resulted in weak or no rescue of the mutant sleep phenotype. Together, these data suggest that SSS expression in cholinergic, but not glutamatergic or dopaminergic neurons, is important for sleep regulation. However, we cannot exclude the possibility that some non–cholinergic neurons also contribute to the strong rescue by *Cha*–Gal4. Like other drivers that rescue well, the *Cha*–Gal4 expression pattern is also anatomically broad, and thus the regulation of sleep by SSS may involve widely distributed neurons of the *Drosophila* brain.

Like *Shaker* mutants, *sss* mutants display rhythmic leg–shaking under ether anesthesia[11],[26]. This leg–shaking phenotype was rescued by SSS expression using the *elav*–Gal4 and *sss*–Gal4 drivers (Fig. 1a). Interestingly, we found that while the cholinergic driver, *Cha*–Gal4, efficiently rescued the sleep phenotype of *sss* mutants, it had little effect on leg shaking. In contrast, expression of SSS in glutamatergic neurons with *vGlut*–Gal4 rescued the leg–shaking phenotype of *sss* mutants, but displayed only weak rescue of the sleep phenotype (Fig. 1b). These data demonstrate that the circuits mediating ether–induced leg shaking and

sleep regulation are distinct, suggesting that the sleep dysfunction in *sss* mutants is not caused by a defect in motor neurons.

SSS and Shaker are enriched in the same brain regions

To investigate a possible cell–autonomous role for SSS in regulating Shaker, we sought to determine whether the two proteins could be colocalized in the adult *Drosophila* brain. To visualize SSS–expressing cells, we generated a new anti–SSS antibody and performed whole–mount immunostaining of adult brains. There was appreciable overlap between the SSS immunostaining and the expression of GFP driven by *sss*–Gal4 (compare Fig. 2 and Supplementary Fig. 1). SSS–specific immunoreactivity was observed in the mushroom bodies and other structures such as the antennal nerves, superior protocerebrum, and the lobula plate of the optic lobes (Figs. 2a,c). Loss of SSS immunoreactivity in *sss* null mutants demonstrates specificity of our antibody (Fig. 2e).

To examine the Shaker expression pattern, we also raised a new Shaker antibody. We found that Shaker and SSS show similar expression patterns, with broad expression throughout the brain, but with clear enrichment in specific structures, including the mushroom bodies, the superior protocerebrum, antennal nerves, and neuronal processes in the lobula plate (Figs. 2b,d). This staining pattern was specific, as it was absent in *Shaker* deficiency ($Shaker^{Df}$; B55/W32)[27] brains (Fig. 2f), and is similar to that found in a previous Shaker immunohistochemical study[28]. The requirement of different fixatives for the anti–SSS and anti–Shaker antibodies prevented a direct assessment of colocalization. However, the finding that SSS and Shaker are enriched in similar regions of the brain suggests that SSS regulates Shaker in a cell–autonomous manner.

Shaker and SSS specifically affect each other's expression

We next used our Shaker antibody to examine the relationship between Shaker and SSS in greater detail. The antibody recognized two bands of apparent molecular weight of ~65–75 kD on Western blots of wild–type fly head extracts, but not in $Shaker^{Df}$ extracts, demonstrating that the antibody selectively reacts with Shaker protein (Fig. 3a). Since alternative splicing produces multiple isoforms of Shaker, the two bands may represent different isoforms. Both Shaker bands were reduced in sss^{P1} mutants, confirming our previous finding that *sss* affects Sh protein expression[11]. In contrast, *Shaker* mRNA levels were not reduced in sss^{P1} mutants (Supplementary Fig. 5), indicating that the reduction of Shaker protein in *sss* mutants is caused by post–transcriptional regulation of Shaker.

Other short–sleeping mutants, such as DAT^{fumin} and Clk^{jrk} [29–31], did not exhibit noticeable reductions in Shaker protein levels (Fig. 3a), demonstrating that reduced sleep is not necessarily linked to a reduction in Shaker expression. In addition, *sss* does not affect expression of all potassium channels, as expression of Eag protein was comparable in *sss* mutants and wild–type flies (Fig. 3b).

To determine whether there is a reciprocal effect of *Shaker* on SSS expression, we examined SSS levels in $Shaker^{Df}$ mutants and found that SSS expression is reduced compared to controls, indicating that Shaker and SSS mutually affect each other's expression. SSS levels

were not reduced in *DAT*^{fumin} and *Clk*^{jrk} mutants (Fig. 3a and Supplementary Fig. 6), providing further evidence for a specific interaction between SSS and Shaker. The mutual effects of SSS and Shaker on each other's expression are consistent with the hypothesis that SSS and Shaker exist in a complex.

Shaker localization is altered in *sss* mutants

Because neuronal output can be regulated not only by the number of ion channels, but also by their regional and subcellular localization, we examined Shaker staining in whole–mount brains. Consistent with the Western blot results in Figure 3, we found that overall Shaker expression was lower in *sss* mutants compared to control flies (Fig. 4b vs. 4a). However, the degree to which Shaker was reduced in *sss* mutants was not uniform across brain regions. For instance, Shaker immunoreactivity in *sss* mutants was greatly reduced in antennal nerves, lobula plate, and certain subregions (e.g., α and α' lobes) of the mushroom bodies, but it was not as severely affected in other subregions (e.g., γ lobes) of the mushroom bodies (Fig. 4b vs. 4a).

Furthermore, the subcellular localization of Shaker appeared to be altered in *sss* mutants. In wild–type animals, Shaker was expressed widely in neuronal fiber tracts. For example, we observed strong Shaker expression in the antennal nerves (Fig. 4a), processes originating from visual projection neurons (Fig. 4c), and the cervical connective (Figs. 4e and 4g). In contrast, in *sss* mutants, we found Shaker predominantly in cell bodies in both brains (Fig. 4d) and thoracic ganglia (Figs. 4f and 4h). Although we cannot rule out the possibility that SSS is more important for Shaker expression in cells where Shaker is predominantly in neuronal processes than in cells where the channel is enriched in cell bodies, our data suggest that SSS is required for proper subcellular localization of Shaker, i.e. targeting to or retention at neuronal processes.

Targeted expression of *sss* restores Shaker expression

To address whether SSS regulates Shaker in a cell–autonomous manner, we first examined whether restoration of SSS in specific brain regions of *sss* mutants selectively rescues Shaker expression in the same regions. We coupled the expression of a *sss* transgene to the OK107– and *vGlut*–Gal4 drivers, which have complementary expression patterns in two brain regions where Shaker is normally enriched. Whereas OK107–Gal4 directed GFP expression to the mushroom bodies but not to a group of visual projection neurons sending processes to the optic lobe, the opposite was true for the *vGlut*–Gal4 driver (Figs. 5a,c,e,g).

Using these drivers to express UAS–*sss*, we found that Shaker expression in *sss* mutants was restored in the regions where GFP, and presumably transgenic SSS, was expressed. Thus, restoration of SSS in *sss* mutants by OK107–Gal4 increased Shaker expression in the mushroom bodies, especially the α and α' lobes (Fig. 5b), but not in the visual projection neurons (Fig. 5d). In contrast, *vGlut*–Gal4 rescue of *sss* enhanced Shaker expression in the visual projection neurons (Fig. 5h) but not in the mushroom bodies (Fig. 5f). While it is possible that SSS exerts local non–cell–autonomous effects on Shaker levels, these data are consistent with a cell–autonomous role for SSS regulation of Shaker expression.

Rescue of SSS function at the neuromuscular junction

We next addressed whether SSS cell–autonomously regulates Shaker function *in vivo* by examining the synaptic signaling properties at the larval neuromuscular junction (NMJ), as a prior study of the hypomorphic sss^{qvr} allele reported that functional properties at the NMJ are altered[32]. Pre– and post–synaptic phenotypes at the NMJ were assayed by measuring spontaneous miniature excitatory junctional potential (mEJP) frequency and the amplitude and kinetics of specific ionic currents, respectively.

The mEJP frequency was significantly increased in sss^{P1} mutant larvae compared to their wild–type control line (Fig. 6a). A similar increase in the mEJP frequency was observed in $Shaker^{Df}$ mutant larvae (Fig. 6a), showing that disruption of either *sss* or *Shaker* leads to similar NMJ phenotypes. The increased mEJP frequency observed in sss^{P1} larvae was abolished by expression of SSS presynaptically using the pan–neuronal *elav*–Gal4 driver. In contrast, consistent with presynaptic release frequency being regulated by glutamatergic motor neurons, expression of SSS in muscle with the 24B– Gal4 driver or in cholinergic neurons with the *Cha*–Gal4 driver failed to reduce the high mEJP frequency in sss^{P1} mutants (Fig. 6a).

The magnitude and kinetics of the Shaker–dependent I_A current in larval muscles was also altered in sss^{P1} mutants (Figs. 6b–d). The sss^{P1} mutation significantly delayed the time–to–peak (t_{peak}) of I_A at 10 mV (Fig. 6b) and also decreased the I_A current magnitude at every voltage ≥ −20 mV (Figs. 6c,d). In contrast, magnitude and kinetics of non–inactivating, Shaker–independent I_K current were not altered in sss^{P1} mutants (Supplementary Fig. 7). The increase in t_{peak} and the reduction in I_A amplitude in sss^{P1} mutants can be rescued by transgenic expression of SSS in muscle with 24B–Gal4, but not in neurons with *elav*–Gal4 (Figs. 6b,d). It should be noted that only a partial rescue of I_A amplitude is obtained with 24B–Gal4. Interestingly, a reduction in I_A current was observed when SSS is overexpressed in muscles of wild–type animals using 24B–Gal4 (Supplementary Fig. 8), suggesting that the presence of excess SSS can impair Shaker function in muscle. Together, the electrophysiological results demonstrate that SSS regulates Shaker function in a cell–autonomous manner in both neurons and muscles.

SSS enhances Shaker channel function

We have shown that SSS is required for normal levels, localization, and activity of Shaker *in vivo*. Bioinformatic prediction of SSS tertiary structure using PHYRE (Protein Homology/analogY Recognition Engine)[33] revealed a single disulfide–bonded domain containing three beta sheet–rich loops (or “fingers”) found in the Ly–6/neurotoxin superfamily of proteins (Supplementary Fig. 9a)[12]. Furthermore, the *sss* gene contains two conserved intron breaks in the coding region shared by Ly–6/neurotoxin gene family members[34] (Supplementary Fig. 9b). The SSS protein also exhibits other features of the Ly–6 domain, such as an N–terminal leucine/isoleucine and a C–terminal asparagine, as well as pairs of cysteine residues with characteristic spacing. Together, these observations suggest SSS is a member of the Ly–6/neurotoxin superfamily. Since many neurotoxins are known to act on ion channels, including Shaker–type K^+ channels[16,35,36], the structural similarity of SSS to neurotoxins

suggests that SSS might be an endogenous “proto–toxin” that binds to Shaker and regulates its activity.

To determine whether SSS affects Shaker channel activity, we co–expressed *sss* and *Shaker* in heterologous cells and examined the effects on Shaker current amplitude and kinetics. We first recorded Shaker currents in human embryonic kidney (HEK–tsA) cells expressing wild–type *Shaker* in the presence or absence of *sss* (Fig. 7). Co–expression with *sss* resulted in faster kinetics of Shaker current, significantly reducing t_{peak} (Figs. 7a,c). A similar effect on the kinetics of Shaker current was observed with co–expression of SSS and wild–type Shaker channels in *Xenopus* oocytes (Figs. 7b,c), whereas amplitude of Shaker current was largely unaffected (Supplementary Fig. 10). Although the conditions used to coexpress *Shaker* and *sss* may not have been optimal to observe an effect on current amplitude, another potential explanation is that an additional component required for regulation of Shaker expression by SSS, which is present in brain and muscle, is missing in oocytes. Taken together with the slower kinetics of I_A current in sss^{P1} mutants (Figs. 6b,c), these findings suggest that SSS enhances Shaker activity *in vivo*.

In order to assess whether SSS and Shaker can physically interact in a complex, we performed co–immunoprecipitation experiments in *Xenopus* oocytes. When both *sss* and *Shaker* were expressed in oocytes, SSS could be co–immunoprecipitated with Shaker (Fig. 7d). This interaction was specific, because SSS was not detected when immunoprecipitations were performed in the absence of Shaker. In summary, these data show that SSS can form a complex with and enhance the kinetic properties of Shaker.

DISCUSSION

We have presented *in vivo* and *in vitro* evidence that SSS is a novel modulator of Shaker expression, subcellular localization, and activity, and thus is an important regulator of nervous system function. While SSS probably modulates neuronal excitability at multiple anatomical loci, dissociation of the neural circuits responsible for sleep and ether–dependent leg–shaking suggests that the role of SSS in sleep regulation is distinct from its effect on motor control. Our data suggest that SSS acts on Shaker in a cell–autonomous manner and that expression of SSS in cholinergic neurons restores sleep in *sss* mutants, although unidentified non–cholinergic neurons included in the *Cha*–Gal4 expression pattern may also be required. Since upregulation of Shaker by SSS in cholinergic neurons presumably decreases excitability and results in increased sleep, excitation of these cholinergic neurons is likely to promote wakefulness in *Drosophila*. Recent studies have demonstrated involvement of monoaminergic signaling and GABA–responsive peptidergic cells in regulating wakefulness in *Drosophila*[21,23–25,30,37–39]. Thus, as in mammals[40], sleep in *Drosophila* is controlled by arousal systems that include distinct populations of cholinergic, monoaminergic, and peptidergic neurons.

We found that SSS and Shaker were enriched in the same regions of the *Drosophila* brain and that SSS appeared to affect the subcellular distribution of Shaker. Thus, in *sss* mutants the distribution of Shaker channels shifts from an enrichment in processes to a predominance in cell bodies in brains and thoracic ganglia. In addition, loss of SSS or

Shaker resulted in a reduction of the other protein, without a concomitant reduction in transcript, suggesting that these proteins stabilize each other in a complex. The reduction in brain Shaker expression in *sss* mutants could be rescued by transgenic expression of SSS. However, we only observed partial rescue of muscle I_A amplitude in *sss* mutants with overexpression of SSS in muscles. Along these lines, we also found that overexpression of SSS in wild–type muscles reduced I_A amplitude, suggesting that the presence of either too little or too much SSS can impair Shaker function, at least at the larval NMJ.

In addition to modulating the level of Shaker, SSS regulates kinetics of Shaker–dependent potassium currents. Kinetics of Shaker–mediated I_A potassium currents in muscle were selectively slower in *sss* mutants, a phenotype that could be rescued by targeted expression of *sss* in muscle. In heterologous cells, co–expression of Shaker and SSS accelerated Shaker currents and resulted in detectable complex formation between the two proteins. Taken together, these data suggest that SSS directly interacts with Shaker to regulate its levels, localization, and activity.

Properties of voltage–gated potassium channels, such as expression level, subcellular localization, and gating characteristics are influenced by a number of associated regulatory proteins including Kvß/Hyperkinetic, KCNEs, KChIPs, and KChAP[41–43]. The *in vivo* relevance of these regulatory proteins is underscored by the finding that mutations in some of the genes encoding them are associated with human diseases, including Long QT syndromes[41,43]. Unlike most other known regulators of voltage–gated potassium channels, which generally interact with cytoplasmic domains of channel proteins, SSS, as a GPI–anchored protein tethered to the plasma membrane, probably interacts with an extracellular domain of the Shaker channel. The predicted structure of SSS is also unlike those of other known endogenous regulators of voltage–gated potassium channels. Bioinformatic analysis predicts that SSS contains a compact disulfide–bonded beta–sheet structure (three–finger fold) found in the Ly–6/neurotoxin superfamily of proteins. This diverse family includes proteins involved in the modulation of receptor function and immune complex formation, as well as snake neurotoxins that bind the extracellular domains of various ion channels at the cell surface[12,13,15,44].

Snake neurotoxins do not have GPI anchors like SSS. However, ER–targeted expression of soluble dendrotoxin, a specific blocker of Shaker–type potassium channels, results in increased surface expression of Kv1.1[17], a mammalian ortholog of Shaker. This finding led Vacher et al. (2007) to postulate the existence of an endogenous toxin–like ER protein that tethers Shaker channels to the ER membrane and with which dendrotoxin competes for binding. SSS may be such an endogenous neurotoxin–like molecule regulating Shaker function and localization. However, rather than retaining Shaker in the ER, SSS appears to increase surface localization of the channel, either through promotion of Shaker trafficking to or retention at the cell surface.

Lynx1, another GPI–anchored neurotoxin/Ly–6 family member found in mammals, binds to and modulates the activity of a ligand–gated ion channel (nicotinic acetylcholine receptor)[34,45]. Thus, regulation of various ion channels by toxin–like GPI–anchored proteins may be an evolutionarily conserved mechanism, and SSS and Lynx–1 may be founding

members of a family of cell–surface proto–toxins that modulate ion channel properties to control neuronal excitability and signaling. Although BLAST analysis with the primary sequence of SSS does not reveal an obvious mammalian ortholog[11], there are a number of mammalian proteins with a Ly–6 domain and a GPI anchor, one of which may represent a functional homolog of SSS.

In summary, we demonstrate that SSS is a novel regulator of Shaker expression, localization, and function *in vivo*. We propose that SSS acts as an endogenous "proto–toxin" that forms a complex with Shaker and promotes its stability and activity at the cell surface. Since dysregulation of channel function causes a number of inherited human diseases, including migraine, epilepsy, and cardiac arrhythmias[46],[47], identification and characterization of additional toxin–like regulators of ion channels may prove to be a fruitful approach for discovering novel treatment options for these diseases.

METHODS

Fly Stocks and Transgenic Fly Lines

All lines used in behavioral experiments, including Gal4 and UAS lines, were outcrossed at least 5 times into an isogenic *white* background (*iso31*) obtained from the Bloomington Stock Center. $Shaker^{Df}$ line was obtained from D. Bushey and B. Ganetzky, and DAT^{fumin} was obtained from K. Kume. eag^{sc29} (#1442), *Cha*-Gal4 (#6793), D42-Gal4 (#8816), OK107-Gal4 (#854), *TH*-Gal4 (#8848), *repo*-Gal4 (#7415), 24B-Gal4 (#1767) and *elav*-Gal4 (#458) were obtained from the Bloomington Stock Center. Sep54-Gal4 and Mai301-Gal4 were obtained from G. Korge, and *vGlut*-Gal4 and *dilp2*-Gal4 were obtained from J. Simpson and E. Rulifson, respectively. Other driver lines were obtained as previously described[19]. sss^{P1} and $sss^{\Delta 40}$ were described previously[11].

Transgenic fly lines carrying either the UAS-*sss* or *sss*-Gal4 construct were generated by standard techniques in the isogenic background *iso31* (Rainbow Transgenics). For the UAS-*sss* construct, the entire coding region of *sss* was amplified by PCR using the following primers: 5′-GAA TTC ACC ATG TGG ACG CAG AGA AAT GCA GTT GG-3′ and 5′-GTC GAC GAG CCT AAC ACT TTC TAT CTG CTG AGC-3′. The PCR product was inserted into the EcoRI and XhoI restriction sites of pUAST, a P-element vector that contains the Gal4 binding sequence, UAS. The *sss*-Gal4 construct contained ~3.5 kb of the *sss* promoter, including the upstream intergenic region and the first and second introns of the *sss* gene. The following primers were used to amplify this region from wild-type genomic DNA: 5′-AAT CTA GAC TTG TAC TCT CAT GCG CTC-3′ and 5′-GCG GAT CCG CCT TGC CAC CCA CC-3′. The PCR product was inserted into the XbaI and BamHI restriction sites of the pPT-Gal transformation vector, upstream of the Gal4 coding sequence.

Antibody Generation

Because our previously-described antibody raised against a peptide antigen poorly recognizes glycosylated SSS[11] and does not produce SSS-specific signal in whole-mount brain samples, we raised a new antibody against glycosylated SSS as the antigen. To produce soluble, glycosylated SSS protein, we inserted the coding region of *sss* minus the C-

terminal GPI-anchor signal into the pAcGP67A baculovirus transfer vector (BD BioSciences) via the following primers: 5′-TAC CCG GGG AAT GTC AAA CGC GAT CG-3′ and 5′-ATC TAG ACT ACT TGT CAT CGT CGT CCT TGT AGT CAT TGC ACA TAT CTT CCT CAC-3′. Since the vector contains an N-terminal signal peptide, the native signal peptide was also removed from the *sss* coding region, and to facilitate purification, a C-terminal FLAG tag was added. Expression and purification of soluble SSS protein was performed at the Protein Expression Facility of Wistar Institute. To ensure proper glycosylation, SSS protein was expressed in High-Five insect cells (Invitrogen). Soluble SSS protein, purified using an anti-FLAG M2 agarose bead column (Sigma), was used to generate a new polyclonal antibody, UPGP69, in a guinea pig (Cocalico Biologicals).

To generate an antibody to Shaker, we used as the antigen a portion of the Shaker protein common to all isoforms fused to glutathione-S-transferase (GST). To generate this fusion construct, 215 amino acids were amplified by PCR using the following primers: 5′-AAG AAT TCA ATT TGC CCA AAT TGA GCA GTC AAG AC-3′ and 5′-AAT CTA GAG TCG ACA AGA TCT GTG ATG TCA GGC ACC TCG TCT TC-3′. The PCR product was subcloned into a modified pGEX vector (GE Lifesciences). GST-Shaker fusion protein was expressed in BL-21 cells (Novagen) and purified using glutathione sepharose beads (GE Life Sciences). After cleavage of GST using thrombin (GE Life Sciences), the Shaker antigen was used to generate a polyclonal antibody, UPR55, in a rat (Cocalico Biologicals).

Western Blot Analysis and Quantitative Real-Time PCR

Fly heads were homogenized and lysed in extraction buffer (20mM HEPES, pH 7.5, 100mM KCl, 20mM β-glycerophosphate, 100mM Na_3VO_4, 10mM EDTA, 0.3% Triton X-100, 1mM DTT, and a cocktail of protease inhibitors) for 15 min at 4°C. SDS sample buffer was added to head extracts and after 5 min of boiling, extracts were loaded onto 4-12% NuPAGE gels (Invitrogen) for SDS-PAGE. Head extracts from seven females were loaded per lane. Antibodies to SSS (UPGP69), Shaker (UPR55), and Eag[48] were used at 1:1000, and antibody to β-Actin (Abcam) was used at 1:8000. Extracts from $Shaker^{Df}$ flies were included in the diluted Shaker antibody solution to reduce non-specific signal. Immunoreactive bands were visualized using enhanced chemiluminescence reagents (Pierce) and X-ray film. Films were scanned (Epson WorkForce 600) and imported into Photoshop 8.0 (Adobe), and the average intensity of each band was quantified using the histogram command. For background correction, the average intensity of the region immediately above or below the band of interest in the same lane was subtracted. To control for loading, the ratio between the signal intensities of the band of interest and the Actin band in the same lane was computed.

Quantitative real-time PCR was performed essentially as described[49] except that the following *Sh*-specific primers were used: 5′-ATT ATC AGA GTG GTG GCC GAC T-3′ and 5′-CGT CTA AAG GGA CAT TGA CCG-3′.

Co-Immunoprecipitation

cDNA encoding the *ShakerD* isoform in a modified pGEM9zf- vector and cDNA encoding *sss* in a modified pBluescript vector were each linearized using NotI and used to generate

cRNA with mMessage mMachine (Ambion). *Xenopus laevis* were handled according to approved protocols and anesthetized by immersion in 0.18% tricaine solution (Sigma). Oocytes were collected and dissociated in 25 mg/ml collagenase (Type I, Sigma) in 50% L-15 medium/50% 10 mM HEPES (pH 7.4) for 45 min at room temperature. Oocytes were then washed with L-15/HEPES, incubated at 18° C overnight and injected the following day with 1.4 ng ShakerD cRNA and either 1.4 ng *sss* cRNA or an equivalent concentration of transcription reaction mixture from which cDNA template was omitted. Following injection with cRNA, oocytes were maintained in L-15/HEPES at 18° C until experiments were performed, 3-4 days later. 20 cells were lysed in extraction buffer (10 mM Tris, pH 7.4, 100 mM NaCl, 5 mM EDTA, 1% Triton X-100, 0.05% SDS, and Complete protease inhibitors (Roche). Precipitates were removed by microcentrifugation at 10,600 RCF for 10 min at 4 C. 5% of supernatants were saved as a control for subsequent Western blotting. The remaining supernatants were mixed with 1 μl antibody to Shaker (UPR55) at 4° C for 2 hrs. 30 μl Dynal protein G-conjugated magnetic beads (Invitrogen) were used to precipitate Shaker-bound protein from solution overnight with shaking. Immunoprecipitates were washed 6 times with 1 ml cold extraction buffer except that Triton X-100 concentration was reduced to 0.5%. Western blotting was performed as above.

Immunohistochemistry

Immunostaining of whole-mount brain samples was performed essentially as described[19], except for the following modifications. For staining with antibody to Shaker, dissected brains were fixed in Bouin's fixative (Fisher) for 20 min at 4°C. For staining with antibody to SSS, brains were fixed in 4% paraformaldehyde in phosphate buffered saline (1.86 mM NaH_2PO_4, 8.41 mM Na_2HPO_4, and 175 mM NaCl) for 30 min at room temperature. Antibodies to Shaker and SSS were used at 1:2000 and 1:3000, respectively. Fluorescent secondary antibodies were used at 1:2000 (Molecular Probes). To reduce non-specific signal, extracts of $Shaker^{Df}$ or $sss^{\Delta 40}$ mutant flies were included as additional blocking agents during incubation with antibodies to Shaker or SSS, respectively. Immunostained brain or thoracic ganglion samples for wild-type and mutant animals were processed at the same time and imaged with the same settings on a Leica TCS SP5 confocal microscope.

Behavioral Assays

Flies were maintained on standard molasses-yeast-cornmeal food at room temperature, and were entrained to a 12-hr:12-hr light:dark cycle for at least two days before being assayed for sleep. 3- to 7-day old female flies were monitored using the *Drosophila* Activity Monitoring System (Trikinetics) at 25°C, and data were analyzed using MATLAB-based (MathWorks) custom software as described[11]. Sleep was identified as periods of inactivity lasting at least 5 minutes[2]. Ether-induced leg shaking was assayed as described[11].

In Vivo Electrophysiology

Wandering third-instar larvae were immersed in a Ca^{2+}-free saline (HL3.1) and dissected to access the neuromuscular junction as described[50]. Recordings were collected from muscle 6 of hemisegments A3-A5 at room temperature (21-23°C)[50] by Sylgard-coated (Dow Corning) electrodes. The voltage-sensing and current-injection electrodes had initial

resistances of 8-20 and 4-10 MΩ, respectively, when filled with a 2 M KCl solution with 10 mM EGTA and a pH of 7.2 (with KOH). The output of the amplifier (OC-725C, Warner) was low-pass filtered at 1-kHz (8-pole Bessel, model 902, Frequency Devices) and digitized using an AD/DA converter (ITC16, HEKA). Data were recorded/stored by PatchMachine and exported to Igor Pro 6.0 (Wavemetrics) for later analysis.

mEJPs were recorded over 2.5 minutes in an HL3.1 saline containing 1.5 mM Ca^{2+} via a single intracellular electrode placed near the mid-point of the muscle. A custom Igor Pro (Wavemetrics) routine based on the NeuroMatic analysis software (www.neuromatic.thinkrandom.com) identified the mEJPs in the record and calculated the average mEJP frequency.

Ionic currents were elicited/recorded in a Ca^{2+}-free HL3.1 solution (with 5 mM EGTA) via two intracellular electrodes placed at opposite ends of the muscle. Muscles were depolarized either from a resting potential of −80 mV to elicit I_A and I_K or after a 200 ms pre-pulse to −20 mV to elicit I_K alone. I/V curves were generated by plotting peak (for I_A) or steady state (for I_K) current densities (nA/nC) against test pulse voltage. Cellular capacitance was calculated by the equation: $I_{ramp}–C(^{dV}/_{dt})=I_{step}$, where I_{ramp} is recorded at a particular voltage during a ramp of $^{dV}/_{dt}$ and I_{step} is recorded at steady state at that voltage. Time to peak was measured at 10 mV.

In Vitro Electrophysiology

Plasmid DNAs in pGWI or pcDNA3 expression vectors coding for *Drosophila* wild-type ShakerB, *sss* and GFP (for identification of successfully transfected cells) were transfected in HEK-tsA cells by FuGENE6 (Roche); inside-out and whole-cell patch-clamp recordings were conducted 2 days following transfection. For both, the extracellular solution contained (in mM): 130 NaCl, 10 KCl, 2 $CaCl_2$, 2 $MgCl_2$, 10 HEPES, 15 glucose, and pH 7.4 (with *N*-methyl-*D*-glucamine (NMG)). The intracellular solution contained (in mM): 140 KCl, 2 $MgCl_2$, 11 EGTA, 10 HEPES, and pH 7.2 (with NMG). Ionic currents were elicited by depolarizing pulses from a holding voltage of - 100 mV. Time-to-peak (t_{peak}) or time-to-half-max ($t_{0.5}$) were measured at 15 mV. There was no correlation between the Shaker current kinetic effects and current magnitude, indicating a specific effect of SSS on Shaker current kinetics. Inside-out and whole-cell patch-clamp experiments were performed using an Axopatch 200A amplifier (Molecular Devices). The amplifier output was filtered at 10 kHz and digitized at 100 kHz through an ITC-16 AD/DA interface (HEKA). Data were collected and analyzed by using Igor Pro.

For *Xenopus* oocyte recordings, cells were prepared and injected with cRNA encoded by *ShakerD* or *sss* as described above, except that 7 pg *ShakerD* cRNA and 14 ng *sss* cRNA were used per cell. Membrane currents were studied by two-microelectrode voltage clamp (Axoclamp-2A, Molecular Devices). The two intracellular microelectrodes (~1 MΩ) were filled with 3 M KCl. Currents were sampled at 10 kHz and filtered at 2 kHz. Shaker currents were recorded in standard saline containing (in mM): 2 KCl, 96 NaCl, 2 $CaCl_2$, 10 HEPES (pH 7.4). Depolarizing pulses were elicited from a holding potential of −70 mV to voltages between −80 and 60 mV in 20 mV increments. P/4 leak subtraction was employed in hyperpolarizing pulses from the same holding potential. Only oocytes with leak currents less

than 50 nA were used. Data collection and kinetic analyses were performed using PClamp9 (Molecular Devices).

Statistical Analyses

The differences in sleep amount or mEJP frequency among multiple genotypes were analyzed with one-way ANOVAs followed by Tukey's HSD tests for post hoc comparisons. For comparison of behavioral and electrophysiological data between pairs of conditions, Student's t-tests (unpaired, two-tailed) were performed with Bonferroni correction for multiple comparisons where applicable. The genetic rescue experiments of the NMJ phenotypes were analyzed with two-way ANOVAs followed by Student's two-tailed t-tests with Bonferroni correction.

Supplementary Material

Refer to Web version on PubMed Central for supplementary material.

ACKNOWLEDGMENTS

We thank I. Levitan, J. Simpson, D. Bushey, B. Ganetzky, E. Rulifson, K. Kume, G. Korge, and the Bloomington Stock Center for providing antibodies and fly stocks. We are grateful to Tanya Ferguson for help with oocyte preparation and Mallory Sowcik and Rong Xu for technical assistance. This work was funded by the following grants: NINDS K08NS059671 and a Burroughs–Wellcome Fund Career Award for Medical Scientists (M.N.W.), T32HL007953 (T.D.), R01GM057654 and R01GM078579 (T.H.), P01AG017628 (A.S. and K.K.), and a University Research Foundation award from the University of Pennsylvania (K.K.). A.S. is an Investigator of the Howard Hughes Medical Institute.

REFERENCES

1. Hendricks JC, et al. Rest in *Drosophila* is a sleep–like state. Neuron. 2000; 25:129–38. [PubMed: 10707978]
2. Shaw PJ, Cirelli C, Greenspan RJ, Tononi G. Correlates of sleep and waking in *Drosophila melanogaster*. Science. 2000; 287:1834–7. [PubMed: 10710313]
3. Nitz DA, van Swinderen B, Tononi G, Greenspan RJ. Electrophysiological correlates of rest and activity in *Drosophila melanogaster*. Curr Biol. 2002; 12:1934–40. [PubMed: 12445387]
4. Anderson MP, et al. Thalamic Cav3.1 T–type Ca2+ channel plays a crucial role in stabilizing sleep. Proc Natl Acad Sci U S A. 2005; 102:1743–8. [PubMed: 15677322]
5. Bushey D, Huber R, Tononi G, Cirelli C. *Drosophila Hyperkinetic* mutants have reduced sleep and impaired memory. J Neurosci. 2007; 27:5384–93. [PubMed: 17507560]
6. Cueni L, et al. T–type Ca2+ channels, SK2 channels and SERCAs gate sleep–related oscillations in thalamic dendrites. Nat Neurosci. 2008; 11:683–92. [PubMed: 18488023]
7. Espinosa F, Marks G, Heintz N, Joho RH. Increased motor drive and sleep loss in mice lacking Kv3–type potassium channels. Genes Brain Behav. 2004; 3:90–100. [PubMed: 15005717]
8. Espinosa F, Torres–Vega MA, Marks GA, Joho RH. Ablation of Kv3.1 and Kv3.3 potassium channels disrupts thalamocortical oscillations in vitro and in vivo. J Neurosci. 2008; 28:5570–81. [PubMed: 18495891]
9. Cirelli C, et al. Reduced sleep in *Drosophila Shaker* mutants. Nature. 2005; 434:1087–92. [PubMed: 15858564]
10. Douglas CL, et al. Sleep in Kcna2 knockout mice. BMC Biol. 2007; 5:42. [PubMed: 17925011]
11. Koh K, et al. Identification of SLEEPLESS, a sleep–promoting factor. Science. 2008; 321:372–6. [PubMed: 18635795]
12. Tsetlin V. Snake venom alpha–neurotoxins and other 'three–finger' proteins. Eur J Biochem. 1999; 264:281–6. [PubMed: 10491072]

13. Greenwald J, Fischer WH, Vale WW, Choe S. Three–finger toxin fold for the extracellular ligand–binding domain of the type II activin receptor serine kinase. Nat Struct Biol. 1999; 6:18–22. [PubMed: 9886286]
14. Huai Q, et al. Structure of human urokinase plasminogen activator in complex with its receptor. Science. 2006; 311:656–9. [PubMed: 16456079]
15. Klein DE, Stayrook SE, Shi F, Narayan K, Lemmon MA. Structural basis for EGFR ligand sequestration by Argos. Nature. 2008; 453:1271–5. [PubMed: 18500331]
16. Albrand JP, Blackledge MJ, Pascaud F, Hollecker M, Marion D. NMR and restrained molecular dynamics study of the three–dimensional solution structure of toxin FS2, a specific blocker of the L–type calcium channel, isolated from black mamba venom. Biochemistry. 1995; 34:5923–37. [PubMed: 7727450]
17. Vacher H, Mohapatra DP, Misonou H, Trimmer JS. Regulation of Kv1 channel trafficking by the mamba snake neurotoxin dendrotoxin K. Faseb J. 2007; 21:906–14. [PubMed: 17185748]
18. Elliott DA, Brand AH. The GAL4 system : a versatile system for the expression of genes. Methods Mol Biol. 2008; 420:79–95. [PubMed: 18641942]
19. Joiner WJ, Crocker A, White BH, Sehgal A. Sleep in *Drosophila* is regulated by adult mushroom bodies. Nature. 2006; 441:757–60. [PubMed: 16760980]
20. Pitman JL, McGill JJ, Keegan KP, Allada R. A dynamic role for the mushroom bodies in promoting sleep in *Drosophila*. Nature. 2006; 441:753–6. [PubMed: 16760979]
21. Chung BY, Kilman VL, Keath JR, Pitman JL, Allada R. The GABA(A) receptor RDL acts in peptidergic PDF neurons to promote sleep in *Drosophila*. Curr Biol. 2009; 19:386–90. [PubMed: 19230663]
22. Foltenyi K, Greenspan RJ, Newport JW. Activation of EGFR and ERK by rhomboid signaling regulates the consolidation and maintenance of sleep in *Drosophila*. Nat Neurosci. 2007; 10:1160–7. [PubMed: 17694052]
23. Parisky KM, et al. PDF cells are a GABA–responsive wake–promoting component of the *Drosophila* sleep circuit. Neuron. 2008; 60:672–82. [PubMed: 19038223]
24. Shang Y, Griffith LC, Rosbash M. Light–arousal and circadian photoreception circuits intersect at the large PDF cells of the *Drosophila* brain. Proc Natl Acad Sci U S A. 2008; 105:19587–94. [PubMed: 19060186]
25. Sheeba V, et al. Large ventral lateral neurons modulate arousal and sleep in *Drosophila*. Curr Biol. 2008; 18:1537–45. [PubMed: 18771923]
26. Kaplan WD, Trout WE 3rd. The behavior of four neurological mutants of *Drosophila*. Genetics. 1969; 61:399–409. [PubMed: 5807804]
27. Tanouye MA, Ferrus A, Fujita SC. Abnormal action potentials associated with the Shaker complex locus of *Drosophila*. Proc Natl Acad Sci U S A. 1981; 78:6548–6552. [PubMed: 16593105]
28. Rogero O, Hammerle B, Tejedor FJ. Diverse expression and distribution of Shaker potassium channels during the development of the *Drosophila* nervous system. J Neurosci. 1997; 17:5108–18. [PubMed: 9185548]
29. Hendricks JC, et al. Gender dimorphism in the role of cycle (BMAL1) in rest, rest regulation, and longevity in *Drosophila melanogaster*. J Biol Rhythms. 2003; 18:12–25. [PubMed: 12568241]
30. Kume K, Kume S, Park SK, Hirsh J, Jackson FR. Dopamine is a regulator of arousal in the fruit fly. J Neurosci. 2005; 25:7377–84. [PubMed: 16093388]
31. Wu MN, Koh K, Yue Z, Joiner WJ, Sehgal A. A genetic screen for sleep and circadian mutants reveals mechanisms underlying regulation of sleep in *Drosophila*. Sleep. 2008; 31:465–72. [PubMed: 18457233]
32. Wang JW, Humphreys JM, Phillips JP, Hilliker AJ, Wu CF. A novel leg–shaking *Drosophila* mutant defective in a voltage–gated K(+) current and hypersensitive to reactive oxygen species. J Neurosci. 2000; 20:5958–64. [PubMed: 10934243]
33. Kelley LA, Sternberg MJ. Protein structure prediction on the Web: a case study using the Phyre server. Nat Protoc. 2009; 4:363–71. [PubMed: 19247286]
34. Miwa JM, et al. lynx1, an endogenous toxin–like modulator of nicotinic acetylcholine receptors in the mammalian CNS. Neuron. 1999; 23:105–14. [PubMed: 10402197]

35. Eriksson MA, Roux B. Modeling the structure of agitoxin in complex with the Shaker K+ channel: a computational approach based on experimental distance restraints extracted from thermodynamic mutant cycles. Biophys J. 2002; 83:2595–609. [PubMed: 12414693]
36. Harvey AL. Twenty years of dendrotoxins. Toxicon. 2001; 39:15–26. [PubMed: 10936620]
37. Andretic R, van Swinderen B, Greenspan RJ. Dopaminergic modulation of arousal in *Drosophila*. Curr Biol. 2005; 15:1165–75. [PubMed: 16005288]
38. Crocker A, Sehgal A. Octopamine regulates sleep in *Drosophila* through protein kinase A–dependent mechanisms. J Neurosci. 2008; 28:9377–85. [PubMed: 18799671]
39. Yuan Q, Joiner WJ, Sehgal A. A sleep–promoting role for the *Drosophila* serotonin receptor 1A. Curr Biol. 2006; 16:1051–62. [PubMed: 16753559]
40. Saper CB, Scammell TE, Lu J. Hypothalamic regulation of sleep and circadian rhythms. Nature. 2005; 437:1257–63. [PubMed: 16251950]
41. Li Y, Um SY, McDonald TV. Voltage–gated potassium channels: regulation by accessory subunits. Neuroscientist. 2006; 12:199–210. [PubMed: 16684966]
42. Misonou H, Trimmer JS. Determinants of voltage–gated potassium channel surface expression and localization in mammalian neurons. Crit Rev Biochem Mol Biol. 2004; 39:125–45. [PubMed: 15596548]
43. Abbott GW, Goldstein SA. Potassium channel subunits encoded by the KCNE gene family: physiology and pathophysiology of the MinK–related peptides (MiRPs). Mol Interv. 2001; 1:95–107. [PubMed: 14993329]
44. Gumley TP, McKenzie IF, Sandrin MS. Tissue expression, structure and function of the murine Ly–6 family of molecules. Immunol Cell Biol. 1995; 73:277–96. [PubMed: 7493764]
45. Ibanez–Tallon I, et al. Novel modulation of neuronal nicotinic acetylcholine receptors by association with the endogenous prototoxin lynx1. Neuron. 2002; 33:893–903. [PubMed: 11906696]
46. Boussy T, et al. Genetic basis of ventricular arrhythmias. Cardiol Clin. 2008; 26:335–53. v. [PubMed: 18538183]
47. Catterall WA, Dib–Hajj S, Meisler MH, Pietrobon D. Inherited neuronal ion channelopathies: new windows on complex neurological diseases. J Neurosci. 2008; 28:11768–77. [PubMed: 19005038]
48. Schopperle WM, et al. Slob, a novel protein that interacts with the Slowpoke calcium–dependent potassium channel. Neuron. 1998; 20:565–73. [PubMed: 9539129]
49. Zheng X, Yang Z, Yue Z, Alvarez JD, Sehgal A. FOXO and insulin signaling regulate sensitivity of the circadian clock to oxidative stress. Proc Natl Acad Sci U S A. 2007; 104:15899–904. [PubMed: 17895391]
50. Feng Y, Ueda A, Wu CF. A modified minimal hemolymph–like solution, HL3.1, for physiological recordings at the neuromuscular junctions of normal and mutant *Drosophila* larvae. J Neurogenet. 2004; 18:377–402. [PubMed: 15763995]

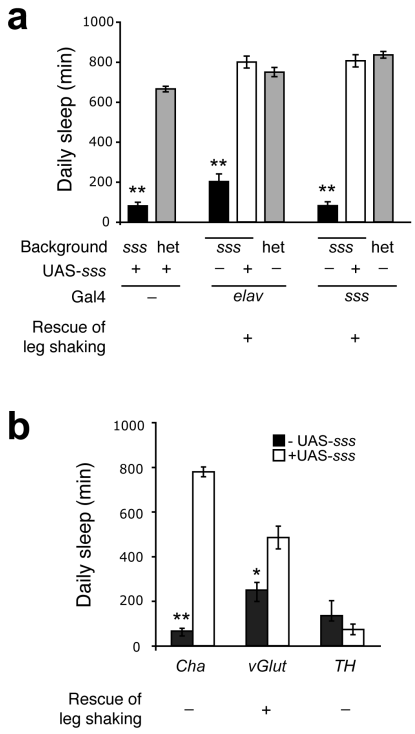

Figure 1.

Rescue of the sleep phenotype of *sss* mutants with a UAS–*sss* transgene (**a**) Daily sleep amounts for female sss^{P1} mutant flies with a UAS–*sss* transgene and either an *elav*–Gal4 or *sss*–Gal4 driver (white bar) were markedly increased relative to sss^{P1} mutants with either the transgene or the driver alone (black bar). Heterozygous (het) sss^{P1} flies served as a wild–type control (gray bar). Successful rescue of ether–induced leg shaking is indicated by "+" at the bottom. In this and subsequent figures, error bars indicate SEM. n ≥ 30 for each genotype. $^{**}P < 0.0001$.

(**b**) Rescue of the sleep phenotype by expression of *sss* in cholinergic neurons. For each Gal4 driver, daily sleep amounts are presented for female sss^{P1} mutant flies carrying either the driver alone (black bar) or for those carrying both the driver and a UAS–*sss* transgene (white bar). Rescue of ether–induced leg shaking is shown for each driver as successful ("+") or unsuccessful ("−"). n ≥ 30 for each genotype, except for *TH*–Gal4 driver control, for which n = 12. $^{*}P < 0.01$; $^{**}P < 0.0001$.

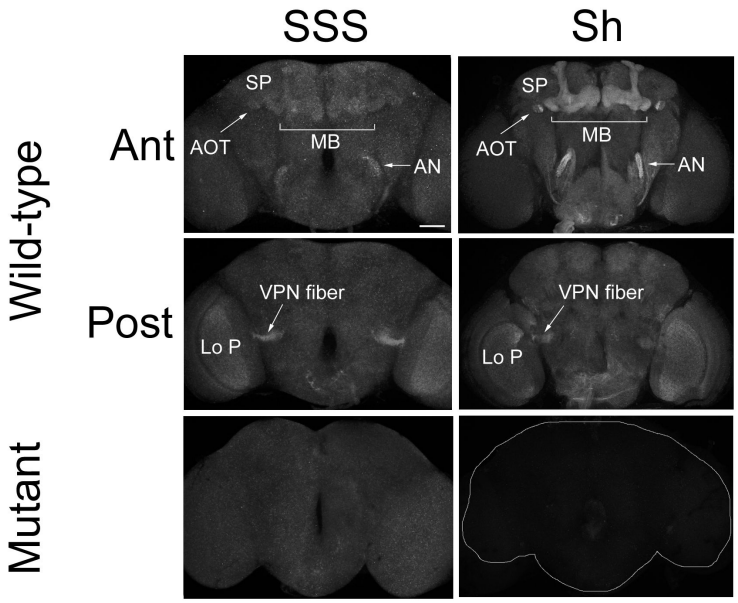

Figure 2.

Distribution of SSS and Shaker immunoreactivity in the adult fly brain Whole–mount brain samples of *iso31* (wild–type– **a**–**d**) flies were stained with an antibody to SSS (**a**, **c**) or to Shaker (**b**, **d**). Appropriate mutant lines ($sss^{\Delta 40}$ for anti–SSS, **e**, and $Shaker^{Df}$ for anti–Shaker, **f**) are also shown. Maximal intensity projections of 1–μm confocal sections of the anterior third (ant–**a**, **b**) or posterior third (post–**c**, **d**) of the brain are shown for wild–type brains. For mutant brains, maximal projections of the entire brain are shown. The bracket and arrows point to the mushroom bodies (MB), anterior optic tubercle (AOT), superior protocerebrum (SP), and the antennal nerve (AN). SSS and Shaker expression in the posterior third of the brain included fibers from a group of visual projection neurons (VPN fiber) sending processes to the lobula plate (Lo P) of the optic lobe. Representative brains are shown, taken from at least three independent experiments. For *iso31* brains, n=21 for anti–SSS and n=12 for anti–Shaker. For $sss^{\Delta 40}$ brains, n=16 and for $Shaker^{Df}$ brains, n=10. Scale bar, 50 μm.

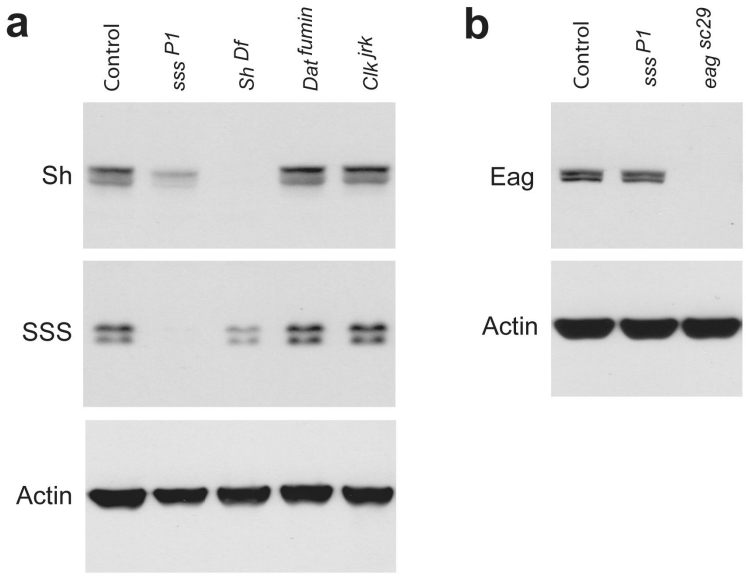

Figure 3.

Shaker and SSS specifically affect each other's expression (**a**) Shaker was reduced in sss^{P1} mutants, and SSS was reduced in $Shaker^{Df}$ (Sh^{Df}) mutants. Shaker and SSS levels were not reduced in other short–sleeping mutants, DAT^{fumin} and Clk^{jrk}. Head extracts of background control and mutant flies of indicated genotypes were analyzed by Western blotting using antibodies to Shaker and SSS. $Shaker^{Df}$ and sss^{P1} mutant flies were used as negative controls, and antibody to Actin was used to control for loading. Representative blots from 4 independent experiments are shown in **a** and **b**.

(**b**) Eag expression was not affected in *sss* mutants. Head extracts of eag^{sc29} and sss^{P1} mutants, as well as background control, were analyzed by Western blotting using antibodies to Eag and Actin (for loading control).

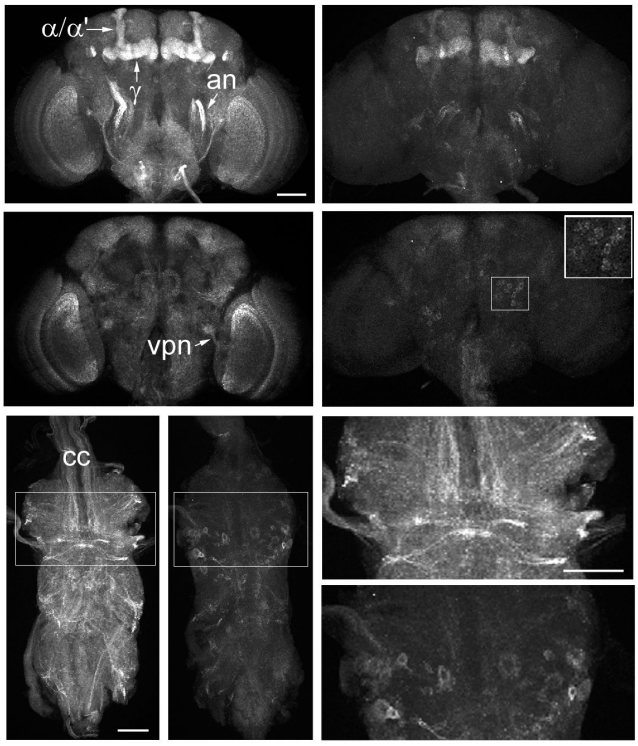

Figure 4.

Altered Shaker expression and localization in *sss* mutants Shaker immunostaining of control *iso31* (**a**, **c**) and $sss^{\Delta 40}$ (**b**, **d**) whole–mount adult brains is shown. Maximal intensity projections from 1–μm sections from the entire brain are shown for (**a**) and (**b**), while a single 1–μm section from the posterior aspect of the brain including the protocerebral bridge is shown for (**c**) and (**d**). A 2x magnified inset is shown for (**d**). Shaker immunostaining in whole–mount adult thoracic ganglia of *iso31* (**e**,**g**) and $sss^{\Delta 40}$ (**f**, **h**). (**g**) and (**h**) are 2x magnified images from the boxed areas in (**e**) and (**f**), respectively. Structures are labeled as follows: alpha and alpha' (α/α') and gamma (γ) lobes of the mushroom bodies, antennal nerve (an), processes of a group of visual projection neurons (vpn), and the central connective (cc). Representative images are shown, from at least three independent experiments. n=10 and n=11 for *iso31* and $sss^{\Delta 40}$ brains, respectively. n=9 for *iso31* and $sss^{\Delta 40}$ thoracic ganglia. Scale bar in (**a**) for (**a**–**d**), (**e**) for (**e**,**f**), and (**g**) for (**g**,**h**), 50 μm

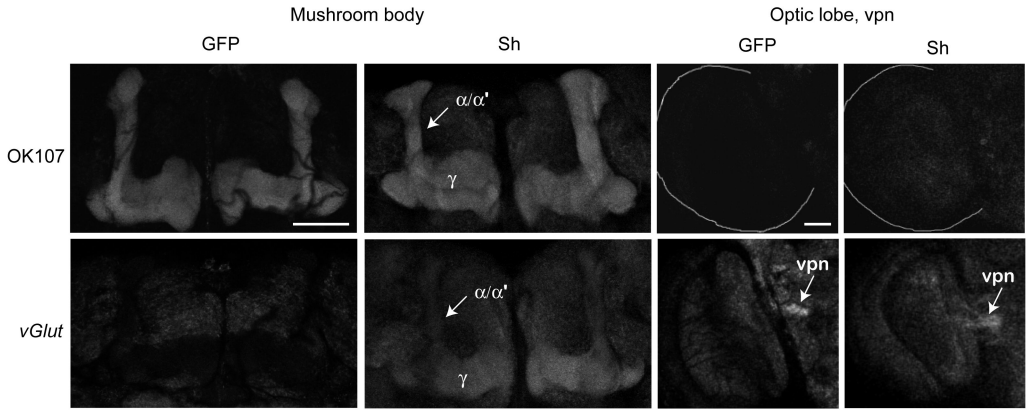

Figure 5.

Rescue of Shaker expression in *sss* mutants by transgenic expression of *sss* (**a**–**d**) OK107–Gal4 was used to direct expression of GFP (**a**, **c**) or *sss* (**b**, **d**), and GFP or Shaker expression was examined, respectively. Since Shaker was enriched in synapse–rich neuropil, GFP fused to *synaptogamin* (*syt*–GFP), which is targeted to the synapse, was used. GFP expression was seen in the mushroom bodies (**a**), but not in the group of visual projection neurons (VPNs) sending processes to the optic lobe (**c**). Transgenic expression of *sss* using OK107–Gal4 increased Shaker expression in the mushroom bodies (**b**), but not in the optic lobe (**d**). (**e**–**h**) *vGlut*–Gal4 directed GFP expression in the visual projection neurons and the optic lobe (**g**), but not the mushroom bodies (**e**). Transgenic expression of *sss* using *vGlut*–Gal4 increased Shaker expression in the optic lobe (**h**), but not in the mushroom bodies (**f**). Arrows point to the fiber bundles formed by the VPNs. Maximal intensity projections of seven 1–μm sections from the anterior of the brain are shown for (**a**), (**b**), (**e**), and (**f**), and a single 1–μm section from the posterior of the brain at the level of the protocerebral bridge is shown for (**c**), (**d**), (**g**), and (**h**). Representative brains are shown, taken from two independent experiments. n=5 or 6 for all genotypes. Scale bar in (**a**) for (**a**,**b**,**e**,**f**) and (**c**) for (**c**,**d**,**g**,**h**), 50 μm

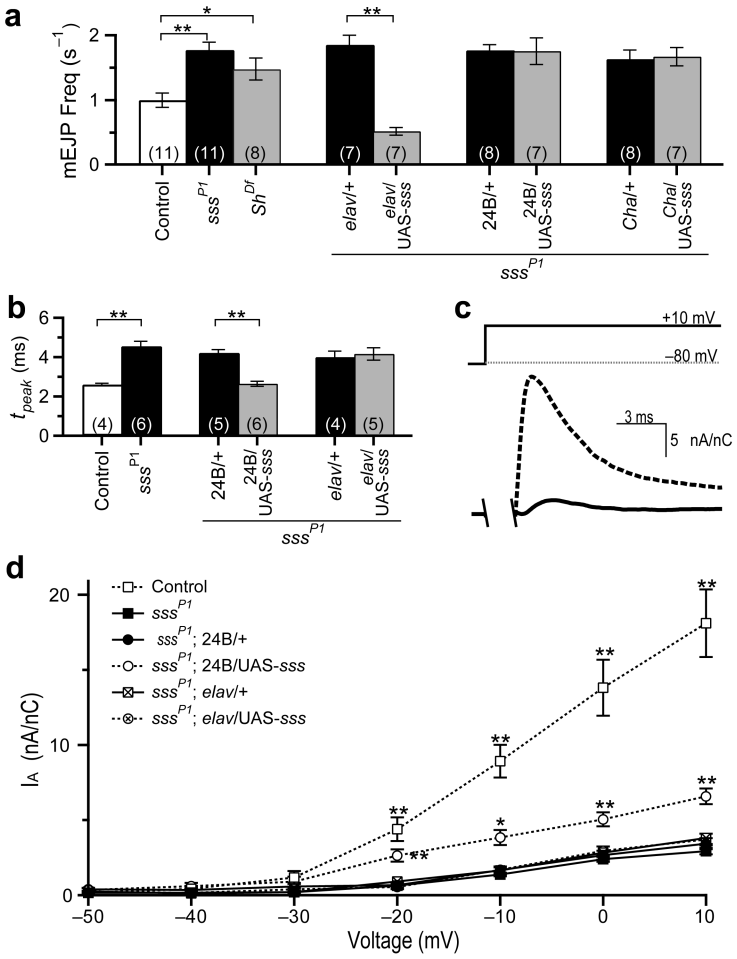

Figure 6.

Cell–autonomous rescue of the *sss* phenotypes at the *Drosophila* larval NMJ (**a**) mEJP frequencies for *sss*^{P1} (black bars) and *Shaker*^{Df} (gray bar) larvae were significantly increased relative to background controls (white bar). The UAS–*sss* transgene (gray bars) significantly decreased mEJP frequencies in the *sss*^{P1} mutant background only when combined with the *elav*–GAL4 driver.

(**b**) Time–to–peak I_A current (t_{peak}) was significantly greater in *sss*^{P1} (black bars) than in background controls (white bar). The UAS–*sss* transgene (gray bars) significantly decreased I_A t_{peak} in the *sss*^{P1} mutant background only when paired with the 24B–Gal4 driver.

(**c**) Representative traces of I_A current illustrating the decrease in current magnitude and delayed time–to–peak in *sss*^{P1} mutant larvae. Dashed line is from wild–type; solid line is from mutant muscle.

(**d**) I_A density in larval muscle could be partially rescued over a range of voltages in *sss*^{P1} mutants bearing a UAS–*sss* transgene under control of the muscle–specific driver 24B–Gal4, compared to background and driver controls. Rescue was not observed using the pan–neuronal driver *elav*–Gal4 coupled to UAS–*sss*. Values for n are the same as in (**b**). *P < 0.05; **P < 0.01.

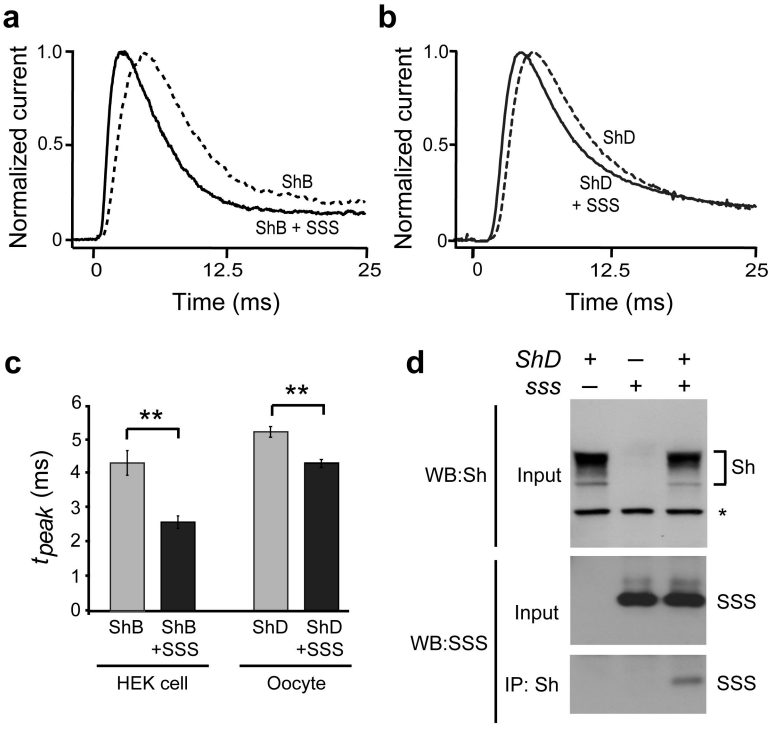

Figure 7.

SSS modulates Shaker function.

(**a**) Representative normalized currents measured at 15 mV from a holding potential of −100 mV in excised patches of HEK–tsA cells transfected with cDNA encoding the *ShakerB* (*ShB*) isoform in the absence or presence of *sss*.

(**b**) Representative normalized currents measured by two–electrode voltage clamp at 20 mV from a holding potential of −70 mV in oocytes expressing the *ShakerD* (*ShD*) isoform in the absence or presence of *sss*.

(**c**) Time to reach peak current (t_{peak}) following a step change to 15 mV from a holding potential of −100 mV in HEK-tsA cells or following a step change to 20 mV from a holding potential of −70 mV in oocytes. n=5 for *ShakerB* alone, n=6 for *ShakerB* + *sss*, n=14 for *ShakerD* alone, n=14 for *ShakerD* + *sss*; $^{**}P < 0.01$.

(**d**) Extracts from oocytes injected with cRNA derived from *ShakerD*, *sss*, or both were immunoprecipitated (IP) with an antibody to Shaker and analyzed by Western blotting (WB) using an antibody to SSS. Prior to immunoprecipitation, 5% of cell extracts (Input) were analyzed separately using antibodies to SSS and Shaker. A non–specific band (*) served as a loading control.